#### **TOPICAL REVIEW • OPEN ACCESS**

# Chemical and structural identification of material defects in superconducting quantum circuits

To cite this article: S E de Graaf et al 2022 Mater. Quantum. Technol. 2 032001

View the <u>article online</u> for updates and enhancements.

# You may also like

- Spin-active defects in hexagonal boron
- Wei Liu, Nai-Jie Guo, Shang Yu et al.
- Quantum information processing with superconducting circuits: a review G Wendin
- Variational quantum compiling with double
- Q-learning Zhimin He, Lvzhou Li, Shenggen Zheng et

# Materials for **Quantum Technology**



#### **OPEN ACCESS**

#### RECEIVED

14 January 2022

#### REVISED

27 May 2022

ACCEPTED FOR PUBLICATION 14 June 2022

PUBLISHED 19 July 2022

Original content from this work may be used under the terms of the Creative Commons Attribution 4.0 licence.

Any further distribution of this work must maintain attribution to the author(s) and the title of the work, journal citation and DOI.



#### **TOPICAL REVIEW**

# Chemical and structural identification of material defects in superconducting quantum circuits

S E de Graaf<sup>1,\*</sup>, S Un<sup>2</sup>, A G Shard<sup>1</sup> and T Lindstróm<sup>1</sup>

- National Physical Laboratory, Hampton Road, Teddington, TW11 0LW, United Kingdom
- Institute for Integrative Biology of the Cell, Department of Biochemistry, Biophysics and Structural Biology, Université Paris-Saclay, CEA, CNRS UMR 9198, Gif-sur-Yvette, F-91198, France
- \* Author to whom any correspondence should be addressed.

E-mail: sdg@npl.co.uk

Keywords: superconducting circuits, decoherence, material defects

#### **Abstract**

Quantum circuits show unprecedented sensitivity to external fluctuations compared to their classical counterparts, and it can take as little as a single atomic defect somewhere in a mm-sized area to completely spoil device performance. For improved device coherence it is thus essential to find ways to reduce the number of defects, thereby lowering the hardware threshold for achieving fault-tolerant large-scale error-corrected quantum computing. Given the evasive nature of these defects, the materials science required to understand them is at present in uncharted territories, and new techniques must be developed to bridge existing capabilities from materials science with the needs identified by the superconducting quantum circuit community. In this paper, we give an overview of methods for characterising the chemical and structural properties of defects in materials relevant for superconducting quantum circuits. We cover recent developments from in-operation techniques, where quantum circuits are used as probes of the defects themselves, to in situ analysis techniques and well-established ex situ materials analysis techniques. The latter is now increasingly explored by the quantum circuits community to correlate specific material properties with qubit performance. We highlight specific techniques which, given further development, look especially promising and will contribute towards a future toolbox of material analysis techniques for quantum.

#### 1. Introduction

That defects in materials can have a negative effect on the performance of electronic devices has been known since the birth of the electronics industry. Much of the materials science developed during the 20th century was motivated by the need for better materials for the semiconductor industry. In these 'classical' devices, material defects usually result in an increased noise level and they can be designed to be nearly impervious to the presence of a small number of defects. Quantum circuits, such as superconducting qubits, differ from their classical counterparts in two important ways: they are sensitive to a very small number of defects (sometimes even single) [1, 2], which not only reduces performance but could also make the device completely inoperable. Quantum circuits thus raise the bar when it comes to the level of control and understanding of the materials that are needed to successfully implement useful circuits, prompting a new paradigm for materials science [3].

The deleterious effects of defects in superconducting circuits have been known and studied for decades [4] and it came as no surprise when they were also seen in the pioneering experiments on superconducting qubits [5–7]. Due to the design and limited coherence of these early circuits the effects were typically seen as broadband charge- or flux noise. However, in later experiments on phase qubits *coherent* coupling to defects in the junction barrier was frequently observed [8]. These experiments unequivocally showed that even a single defect could strongly couple to, and interfere with the operation of, qubits and other quantum circuits. They also showed that these defects, whatever their origin, could behave as prototypical two-levels systems

(TLSs), that is, systems that can be modeled as having two possible configurations separated by an energy difference  $2\Delta$  and connected by a tunneling energy  $\Delta_0$ . It was already well known that lossy dielectrics and other glassy systems could be modeled as a *bath* of effective TLS [9], which couple via strain and dipole moment. The resulting phenomenological standard tunneling model was shown to be consistent with experiments [10, 11], and it became obvious that for qubits the properties and location of *individual* TLS mattered. Today this small number of strongly coupled defects constitutes a major problem in terms of device stability and scaling.

In these early experiments, it was often assumed that most TLS defects were located in the Josephson junction barrier and were caused by a charged atomic-scale defect that could occupy one of two positions in the lattice. Experiments indicated that the average areal density of the resulting TLS was constant for a given fabrication process. This motivated early 'engineering' work to shrink the junction area, which resulted in improved performance. However, targeted materials and interface improvements by early attempts in, for example, growing epitaxial barriers [12] gave little or no benefit.

Fast-forwarding to the current state-of-the-art, this general trend persists. Clever device engineering has succeeded in eliminating many of the materials that host TLS. For instance, by the removal of lossy substrates or by diluting electric fields in critical areas of the device [13–15]. This has resulted in a remarkable improvement in coherence times, with the dominant contribution now coming from TLS residing at surfaces and interfaces that are notoriously hard, if not impossible, to remove, as they are part of the metal—air interfaces of electrodes essential for realising the devices themselves. This means we are approaching the end of the improvements that can be achieved using the aforementioned engineering advances. To further increase coherence times, remaining TLS must be removed or passivated, either by new processing steps or clever chemistry. However, in order to efficiently find such mitigation strategies, the nature of the remaining TLS defects must be understood [1, 16, 17].

There exists a plethora of surface analysis techniques that are routinely used to obtain compositional, structural and chemical information about materials. The superconducting circuit community is now increasingly exploring these techniques in an attempt to correlate material properties with qubit performance. An unfortunate (and perhaps unavoidable) issue is that this task is often very tedious due to the need for a large number of device measurements to obtain statistically meaningful data, in particular in superconducting qubits where device parameters can fluctuate wildly over time due to TLS [2, 18–20]. Thus, 'solving' the TLS problem will require new advances in materials science and new techniques developed specifically for the quantum era. Here, we will give an overview of a number of possible routes to advance our understanding about the chemical and structural nature of TLS defects.

Many different possible origins of the two-level systems seen in quantum circuits have been proposed, and TLS may also be linked (directly or indirectly) to other types of defects, such as magnetic impurities or paramagnetic species, that are generally thought to be responsible for flux noise, another source of decoherence. While this article mainly focuses on methods for revealing the chemical and structural origin of TLS defects, much of what is discussed is potentially also applicable to understanding other types of decohering defects, e.g. sources of flux noise.

Figure 1(a) shows a diagram of the typical layers that are present for a metal deposited onto a substrate. All these layers may host TLS and other types of material defects. In order to understand that a defect is indeed a TLS, we need to probe them as they appear in superconducting circuits. However, as illustrated in figure 1(b) energies and system size accessible by established surface analysis techniques does not yet extend to the regime of TLS. Fundamentally, studying TLS in superconducting quantum circuits is a particularly challenging task for the materials science community because of the following points.

- (a) TLS defects have very low energy scales: a few  $\mu$ eV for defects that couple coherently to qubits, and several orders of magnitude less for excitations in the bath of thermal fluctuators surrounding the coherent TLS (figure 1(b)) [1].
- (b) The defects appear mainly in disordered (structurally and chemically) materials and are thus expected to have many different origins; there are in reality multiple mechanisms in a given material system that can result in (effective) TLS being created.
- (c) The density of defects is also very low, from around  $10^{17}$  cm<sup>-2</sup> for paramagnetic defects responsible for flux noise [21, 22] down to about a single defect per GHz per micrometer of device perimeter [23, 24] (which translates to a handful of resonantly coupled TLSs in a  $100 \times 100 \ \mu m^2$  sized transmon qubit).
- (d) An increasing number of experiments and theories point towards very light elements and molecules (such as hydrogen) [21, 25–29] reacting with or absorbing onto surfaces as possible origins.

No single method exists today that can be applied to meet this challenge; existing and new methods will need to be further developed in order to fully understand the materials for the quantum era.

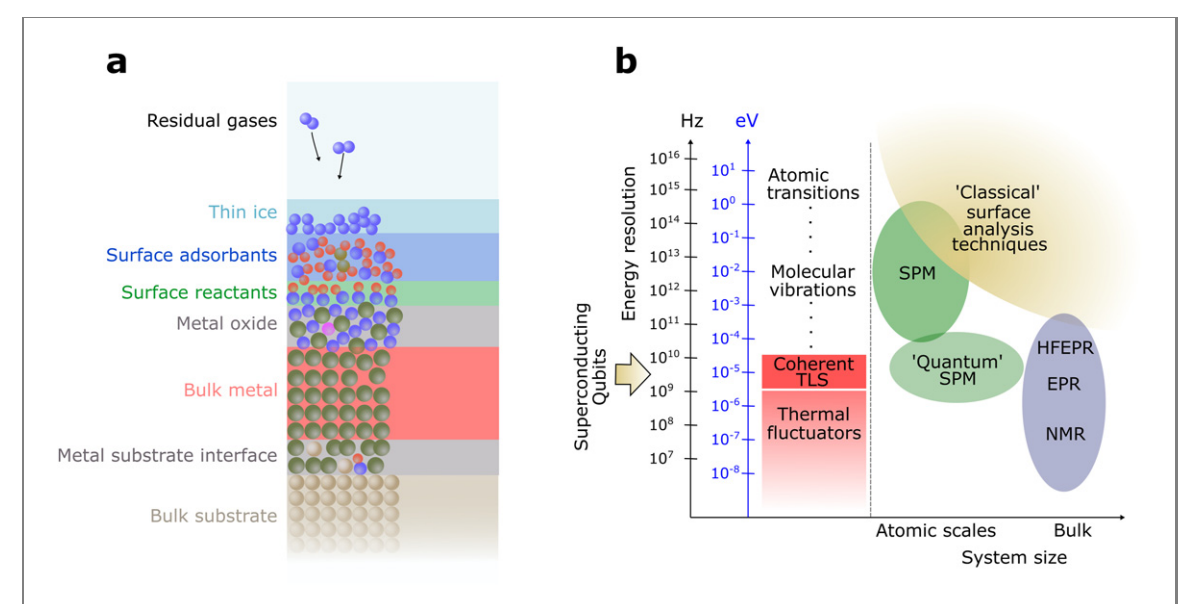


**Figure 1.** (a) Typical layers fabricated and formed in a superconducting circuit (not to scale) that all needs to be understood from a materials and defect point of view. (b) Relevant energy scales and how selected materials analysis techniques compare. Coherent TLSs are those defects that couple strongly to superconducting circuits and they are influenced by a bath of low-energy thermal fluctuators.

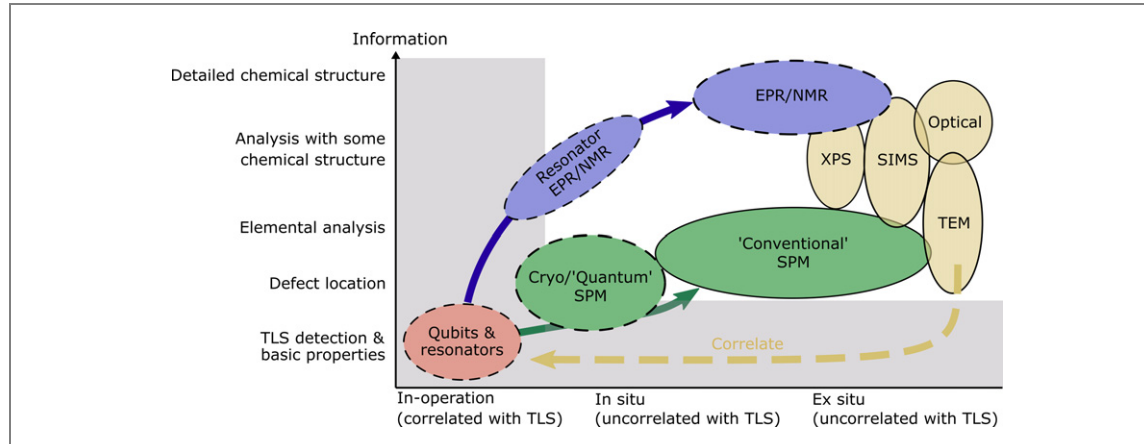


**Figure 2.** Diagram of material analysis techniques towards understanding TLS defects as a function of information content and operating conditions. Established groups of surface analysis techniques (yellow) at present used to correlate properties with qubit performance. Some emerging or established techniques may be further advanced in the future to bridge the gap towards direct TLS identification and chemical analysis (dashed borders). We specifically identify two possible routes: through EPR/nuclear magnetic resonance (NMR) and through scanning probe instrumentation.

Here, we give an overview of recent efforts to obtain structural and chemical information about TLS in superconducting quantum circuits, exploring the possibility of bridging *in situ* defect detection techniques with modern-day *ex situ* surface science techniques, and we discuss the potential of established and emerging material analysis techniques to obtain both direct and indirect (correlated with device performance) information relevant to understanding the nature of TLS. Figure 2 shows specific routes for understanding TLS discussed in the following sections, and highlights the gap that the materials and superconducting quantum device communities need work together to bridge. The rest of this paper is organized as follows. First, in section 2, we discuss the relevant materials used for superconducting quantum circuits. In section 3, we discuss how information about TLS can be obtained from comparative device treatments. In section 4, we outline how 'conventional' materials science can be used to indirectly correlate material properties with device performance. We then highlight two possible routes, which could directly link in-operation TLS detection with chemical or structural information. In section 5, we discuss electron paramagnetic resonance (EPR) techniques and in section 6, techniques capable of directly interrogating individual TLS within quantum devices using scanning probes.

Finally, we point out that this article is not intended to be an all-inclusive review. Instead, our intention is to highlight the challenges that are facing the superconducting circuits and materials science communities and to provide a perspective on potential solutions to these challenges. To this end, we also provide a broad set

of references for the interested reader as a starting point for further exploration of a wider range of topics in materials science.

# 2. Materials for superconducting qubits

To date, work aimed at understanding TLS in superconducting quantum circuits has focused on a handful of metals and their oxides. This is motivated by the nearly total domination of a single fabrication technology, high-quality Josephson junctions based on shadow evaporated  $Al/AlO_x/Al$  devices, deposited either on high resistivity silicon or sapphire  $(Al_2O_3)$  substrates. This technology has been extensively refined over recent decades and yields remarkably reproducible junctions, and its success has meant that research on other material systems is scarce. Alternative materials are most notably AlN, which gives decent coherence times but is ultimately limited by the piezoelectricity of the material [30].  $Nb/AlO_x/Nb$  trilayer junctions is also a well-established technology and gives highly reproducible critical currents exploited in many applications. However, to date, high-coherence qubits have not been demonstrated [31]. Recent advances using the Nb/a-Si/Nb trilayer process could potentially reach long coherence times [32]. Other material platforms are increasingly explored, including more structurally well-defined van der Waals materials [33, 34].

Surrounding circuitry (such as microwave resonators, ground planes and transmon shunt capacitors) is commonly implemented either with the same Al or using Nb- or Ti-based superconductors (Nb, NbN, NbTiN, TiN), which all exhibit various degrees of oxidation of exposed surfaces. Recently, tantalum [35, 36] and TiN [37] were shown to support very high coherence qubits. It is believed that this is related to the improved properties of the surface oxide, but more research is needed to understand the detailed mechanism.

The surfaces and interfaces of these metals is where most remaining detrimental defects reside, either within native oxides or as part of surface adsorbants or contaminants. Despite Al<sub>2</sub>O<sub>3</sub> being one of the most extensively studied oxide surfaces due to its vast number of technological applications [38], a very limited amount of this knowledge has been transferred to the qubit community so far. Much of this can again be attributed to the unprecedented sensitivity to defects that qubits have, and the complications that the disordered native oxide poses in terms of materials analysis.

# 3. Understanding TLS ensembles from device treatments

One way to understand how TLS emerges in these materials is to study the same device (or identical devices) before and after some specific treatment or change to the fabrication process. A major challenge with this approach is that the base variability in measured device performance [2, 19] is often large enough to obscure subtle effects of any treatment, meaning that a large number of devices should be measured [15] to obtain sufficient statistics. Nevertheless, a large number of works have used this approach with varying degrees of success. Some recent examples include correlating *in situ* treatments with qubit coherence times [39, 40], 1/f flux noise [21] in superconducting quantum interference devices (SQUIDs) and resonator loss and noise [25, 41]. We refer to a recent review [1] for a more extensive overview of this approach.

While this type of study can provide new information about TLS, in retrospect very little improvement has been made in the last decade in terms of actual materials quality as quantified by the dielectric loss tangent for the dielectrics [29]. To address this challenge, significant resources are needed to improve measurement throughput, measurement reliability and to allow the exploration of a wide range of treatments.

#### 4. Surface analytical materials science to understand defects

Another approach, with an increased focus in recent years, is to utilise *ex situ* surface analysis techniques to obtain chemical and structural information about materials present and potentially correlate this information with qubit coherence. Here, we summarize these techniques and some lessons that can be learnt from the surface science community.

#### 4.1. Surface analysis applied to superconducting quantum circuits

Surface analytical methods are commonly used to measure the chemical and electronic properties of surfaces. One of the major motivations for their development is to provide information on contaminants, dopants, layer structures and the density of states in electronic materials. The most common laboratory methods for chemical analysis are x-ray photoelectron spectroscopy (XPS) and secondary ion mass spectrometry (SIMS). Related to XPS are Auger electron spectroscopy (AES), reflection electron energy loss spectroscopy (REELS) and angle-resolved photoemission spectroscopy (ARPES). Ion scattering methods, such as low-energy ion scattering,

medium-energy ion scattering and Rutherford back-scattering (RBS) are also occasionally employed. These surface analysis methods provide information from the top few nanometres of a material due to the range of electrons and ions in matter.

XPS uniquely identifies chemical elements through the detection of core-level photoelectrons, the precise position and energy dispersion of which can be related to the chemical environment of the element. The major advantages of the method are a wide applicability to all types of material, the chemical state specificity, and a straightforward route to quantification. Disadvantages include a low sensitivity for the lightest elements, hydrogen cannot be detected due to the lack of core-level electrons, and limits of detection that are typically at the parts-per-thousand level [42]. AES has similar sensitivity limits and, because a focussed electron beam is used to excite Auger emission, cannot be used on materials that will damage easily. Nevertheless, it can be used to assess the cleanliness of surfaces [43] and has excellent spatial resolution [44]. Both ARPES [45] and REELS are primarily used to investigate the electronic properties of materials. Although this information can be tied to chemical structure, it is not straightforward. The direct detection of hydrogen at surfaces is possible through elastic scattering of electrons in REELS [46], where there is a small change in the scattered electron energy from light elements, which at high electron energies is analogous to RBS [47].

XPS is now commonly used to identify the presence of superconductor surface oxides in qubit circuits. Recent works include investigating the presence of Nb [48–50], NbTi [51], NbTiN [13], TiN [52], Al [52] and Ta [35, 36] oxides, and how the oxide regrows [50]. The oxide presence, processing steps or surface treatments can then be correlated with resonator quality factor measurements [49, 50, 52, 53].

SIMS is a highly sensitive surface chemical analysis method that has the typical capability to detect all elements at the parts-per-million level. For semiconductors, metals and minerals, SIMS is employed to detect and locate trace elements, and highly focussed primary ion beams can map the location of these elements with spatial resolutions in the order of 50 nm. The ion beam may also be used to remove layers of material and create depth profiles with typical depth resolutions of a few nanometres. The detection of trace hydrogen in minerals has been demonstrated [54]. The general applicability of SIMS relies upon an understanding of the ionization probability of ejected material. Thus, the technique is extraordinarily sensitive to easily ionized species but can be orders-of-magnitude less sensitive to others. These effects mean that reference materials are required for accurate measurements of composition and to locate interfaces in depth profiles. SIMS has, for example, been used to analyse the composition of surface oxides, contaminants and interfaces for superconducting resonators and qubits [25, 55, 56] as well as 3D detector cavities in the quantum regime [57]. The technique is particularly useful for identifying interdiffusion of materials in multilayer quantum circuits [58]. SIMS has also been used to identify spurious hydrides and carbides [59, 60] at interfaces in Nb devices.

One limitation is that many of the above techniques operate in ultra-high vacuum (UHV) and therefore are of limited use for analyzing surface layers forming in ambient conditions. X-ray absorption spectroscopy (XAS) and similar derived techniques can to some extent address these issues by operating at higher pressures and electron detection offers surface sensitivity. However, instead they require synchrotron radiation for enhanced resolution.

In addition to the above surface sensitive techniques there have been extensive studies attempting to shed light on junction and interface quality by utilising cross-sectional transmission electron microscopy (TEM) imaging of devices. For example, TEM was used to study the amorphous structure of atomic layer deposition (ALD) grown AlO<sub>x</sub> [61], revealing structural metrics, such as stoichiometry, pair distances, and coordination environments in the AlO<sub>x</sub> films, as a function of deposition temperature consistent with changes in the surface hydroxyl density on the growth surface. A number of studies have investigated Al tunnel junctions using TEM to measure the density of defects and pinholes as a function of deposition and fabrication conditions [62-66], and studies have also been combined with low-temperature dielectric capacitance measurements, which are sensitive to TLS present in the dielectrics [64]. The morphology and interface quality can in this way be correlated with deposition conditions and ensemble TLS properties. TEM in combination with different fabrication conditions has also been shown to reveal ensemble TLS properties via resonator loss measurements [67]. TEM is also useful in the development of epitaxial substrate interfaces [68], and derived techniques, such as convergent beam electron diffraction, can reveal local strain in crystals, which is of relevance for TLS. Worth mentioning here is also electron back-scattered diffraction, a SEM-based analogous technique, which avoids any structural damage induced by the preparation of TEM samples. Electron energy loss spectroscopy (EELS) is a useful technique for investigating interfaces for information on local chemical composition and bonding mechanisms [49, 64]. It has been applied to study the influence of substrate treatments, where the presence of oxides can be correlated resonator loss, most notably recently carried out for Al [41] and Nb [48, 49, 69]. Alternatively, x-ray fluorescence and AES could also be used for chemical composition and are typically much more efficient than EELS.

Recently, a combination of several techniques has been applied in more elaborate attempts to correlate material properties with qubit coherence. Nb films used for superconducting qubits were investigated using

cryogenic TEM, atomic force microscopy (AFM) and SIMS to reveal the formation of Nb hydride precipitates [60], a well-known phenomenon for 3D detector Nb cavities [70, 71]. Nb hydrides possibly contribute to both TLS and quasiparticle losses. XAS and x-ray magnetic circular dichroism were used to study cryogenic surface adsorption on Al and Nb films, *in situ* correlating the presence of adsorbants and various surface pre-treatments with SQUID 1/f flux noise magnitude [21]. XAS was also used to reveal the nature of magnetic impurities in the oxide layer of Nb films [72, 73]. XPS combined with resonant inelastic x-ray scattering, using a synchrotron x-ray source, was used to investigate the composition of Nb surface oxides in transmon circuits, revealing a correlation between qubit relaxation times and grain size, grain boundary oxygen diffusion and the amount of near-surface oxides [74]. Combining XPS with TEM and EELS [49] or RBS [75] can provide further details about the structure and presence of surface oxides and the composition of materials [75]. High-coherence tantalum circuits were also recently studied by x-ray diffraction, energy-dispersive x-ray spectroscopy, TEM, XPS and AFM [35].

In summary, many well-established techniques can reveal the presence of unwanted materials on surfaces and interfaces within devices. However, in order to correlate these observations with device coherence extensive comparative studies are required, as none of these methods operate *in situ* with TLS resolving power, and some are destructive in the sense of removing material or implanting others. Nevertheless, they can reveal correlations between material properties and device performance, which can be suggestive of what imperfections *might* pose as TLS. To explore these correlations the materials science community will need to be deeply engaged with the qubit community in increasingly elaborate studies. At the same time, more efficient ways of benchmarking the material quality from in-operation measurements of high-coherence quantum circuits will need to be developed to be able to attribute subtle variations in average device performance with different material properties.

#### 4.1.1. Learning from other areas of materials science

Within the surface science community it is well known that any sample that is exposed to ambient conditions will, apart from reacting with atmospheric gases, soon be covered in layers of water and hydrocarbons. These species may react with the device surface, producing a complex layer of surface-reactive species as well as layers of more weakly bound (physisorbed) species (figure 1(a)). As an example, Al<sub>2</sub>O<sub>3</sub> (and its amorphous oxide unavoidably present in superconducting quantum circuits) has often been studied in depth for various other applications in physics and chemistry. Based on this, it is well known that the Al<sub>2</sub>O<sub>3</sub> surface undergoes hydroxylation upon exposure to ambient [76], resulting in an OH-terminated surface. Sum frequency generation (SFG), second harmonic generation (SHG) and sum-frequency vibrational spectroscopy (SFVS) are examples of ultrafast optical spectroscopy techniques that have been used to study hydroxylated Al<sub>2</sub>O<sub>3</sub> [77]. Selection rules forbid SFG and SHG generation from centrosymmetric environments. In simple materials these signals are only generated from interfaces or regions with strong electric fields. In SFVS, the dipole moments of the oscillators must, on average, have a net orientation to be detected. Other examples include XPS for studying hydroxylated Al<sub>2</sub>O<sub>3</sub> surfaces [38], and using environmental TEM to study the native aluminium oxide growth in real-time [78].

For hydroxylation of  $Al_2O_3$  many reaction pathways compete [79], and for native amorphous  $AlO_x$  we thus also expect many 'defects' in the hydroxylated surface. Some of these defects may form TLS. Due to the strong hydroxylation and binding of water to the  $Al_2O_3$  surface, the amorphous disordered native oxide in qubits is likely to host a cocktail of various defects caused by this hydroxylation chemistry [80], expected to be similar for many other metal-oxide compounds. Much of the relevant surface chemistry likely occurs due to exposure of circuits to ambient conditions when out from the vacuum of processing tools. However, even at lower pressures reactions can take place with residual gases.

#### 4.1.2. Residual gases

Residual gases are of considerable concern to surface analysts. There are continual collisions of gas molecules with all surfaces exposed to the vacuum with a rate per unit area that is proportional to the pressure. These molecules will stick to the surface if the energetic conditions are favourable, as described by the Hertz–Knudsen equation. A typical estimate for the number of atoms in a monolayer is  $10^{19}$  m<sup>-2</sup> and the collision rates are such that, if all gas molecules stick to a surface, this number is reached in approximately 1 s at  $10^{-6}$  mbar pressure. Consequently, amongst others, UHV equipment is used to achieve  $<10^{-9}$  mbar to ensure reactive surfaces remain clean long enough for experiments to be performed. Typical residual gases in baked UHV systems include hydrogen, carbon monoxide and carbon dioxide, and in unbaked or leaky vacuum systems water, hydrocarbons, oxygen and nitrogen are also present. Below 5 K all these gases will stick to surfaces and the cryostat itself becomes a pump reducing the pressure further. Pressures as low as  $10^{-15}$  mbar may be achieved in this way [81] with a monolayer formation time of  $\sim$ 30 years.

Nevertheless, the cryogenically pumped species will coat all cold surfaces, resulting in a constantly changing surface in terms of its strain, magnetic, electric and dielectric environment. This in-operation absorption of species may contribute to TLS energy fluctuations or they may even act as a source of TLS. To prevent a continual time-dependent growth of such thin ice layers on the surface of devices the vacuum system itself requires careful consideration. Leaks can occur through seals (e.g. Viton o-rings) and through the pumping system (turbo-molecular pumps have a low pumping efficiency for hydrogen). Even at  $10^{-15}$  mbar one residual gas molecule will hit the  $\sim 100 \times 100$  nm² interaction area [82–84] of a TLS once every few minutes, and while typically enclosed in many layers of shielding, pressures in excess of  $10^{-15}$  mbar are expected within the sample volume in a typical dilution refrigerator with leaky o-ring seals.

Whilst there are many methods of identifying and detecting the presence of these layers it is rare for them to be employed in operational conditions. Surface analysis at liquid helium temperatures has been performed [45], typically to examine electronic structure but always within ultra-clean systems to prevent surface layers forming. Ellipsometry is a possible means of observing the thickness of contaminant layers on devices *in situ*. This method relies upon the change in polarisation of light reflected from a surface to measure average overlayer thicknesses with a precision better than 0.1 nm. However, optical access to the device, or a witness surface close to the device is required.

# 5. Chemical identification by magnetic resonance

One of the most powerful techniques to date that can reveal both chemical and structural information about individual species from a larger ensemble of defects is EPR, the concept of which is illustrated in figure 3. Paramagnetic species present in a device could be directly linked to flux noise. However, it is needless to say that a detected unpaired electron present in a device could also constitute a charge dipole. Thus, EPR also has direct relevance for understanding TLS either directly or via spins that are influenced by TLS in their vicinity [82, 85–87], linking the associated spin to a chemical entity or environment.

NMR or EPR (and derivatives thereof) are two unique techniques in the sense that they access extremely low energy scales, down to MHz, well below TLS energies, as sketched in figure 1(b). They are at the same time capable of revealing very detailed structural and chemical information.

## 5.1. In situ EPR

EPR using superconducting resonators made of the same materials as in qubit circuits has over the last decade become a fairly well-established technique [88]. However, the main focus so far has been on using planar resonators to couple to well-defined spin systems for quantum memories and similar applications [89]. This is due to to the very long coherence times of certain spin systems and sensitivity down to just a handful of spins [90]. However, the spins that plague superconducting qubit circuits are much more poorly behaved (short coherence times) and present in much smaller numbers, making them impractical for applications. Hence, studies that detect these bad spins are still very scarce [25, 91, 92]. On the other hand, paramagnetic centers present in common semiconductor materials have been thoroughly studied, driven by the needs of the semiconductor industry. This includes, for example,  $P_b$ - and E'-centers at Si/SiO<sub>2</sub> interfaces [93, 94] whose densities affect semiconductor device performance. Much less is known about the surface spins on materials for superconducting quantum circuits (e.g. AlO<sub>x</sub>), although  $P_b$ -centers have also been found at the HF-treated Si(100)/Al<sub>2</sub>O<sub>3</sub> interface [95]. To understand the chemistry of these defects the community needs to focus on developing EPR techniques that can *in situ* reveal information about surface spins in these materials. By repeated surface treatments it can then be possible to find ways to passivate and study the underlying chemistry of defects [25].

#### 5.2. High-field, multifrequency EPR

One drawback of *in situ* measurements of devices is that they are typically limited to low magnetic fields, which limits their resolving power and, consequently, have inherently low information content. These limitations can be overcome by multifrequency EPR. Here, we use multifrequency as shorthand to mean microwave excitation/detection frequencies from conventional  $10-30~\rm GHz$  range to beyond  $300~\rm GHz$  and magnetic fields extending from 1 to well beyond  $10~\rm T$ . The use of multiple frequencies and fields allow increased resolution and separation of field-dependent (electron and nuclear Zeeman) and independent (exchange, zero-field and nuclear hyperfine) magnetic spin interactions, as sketched in figure 3 for a fictitious defect. For example, recent  $3-10~\rm T$  EPR measurements on  $\alpha$ -Al $_2$ O $_3$  single crystals resolved three different radical centers (electron spin species with g-factor  $\sim$ 2.0) [96]. High-field pulsed EPR-based nuclear hyperfine spectroscopy could identify one of the radicals as surface species through their couplings to multiple protons. These surface radicals simultaneously experience both strong and weak proton hyperfine interactions that could only occur on the hydroxylated and protonated  $\alpha$ -Al $_2$ O $_3$  surface.

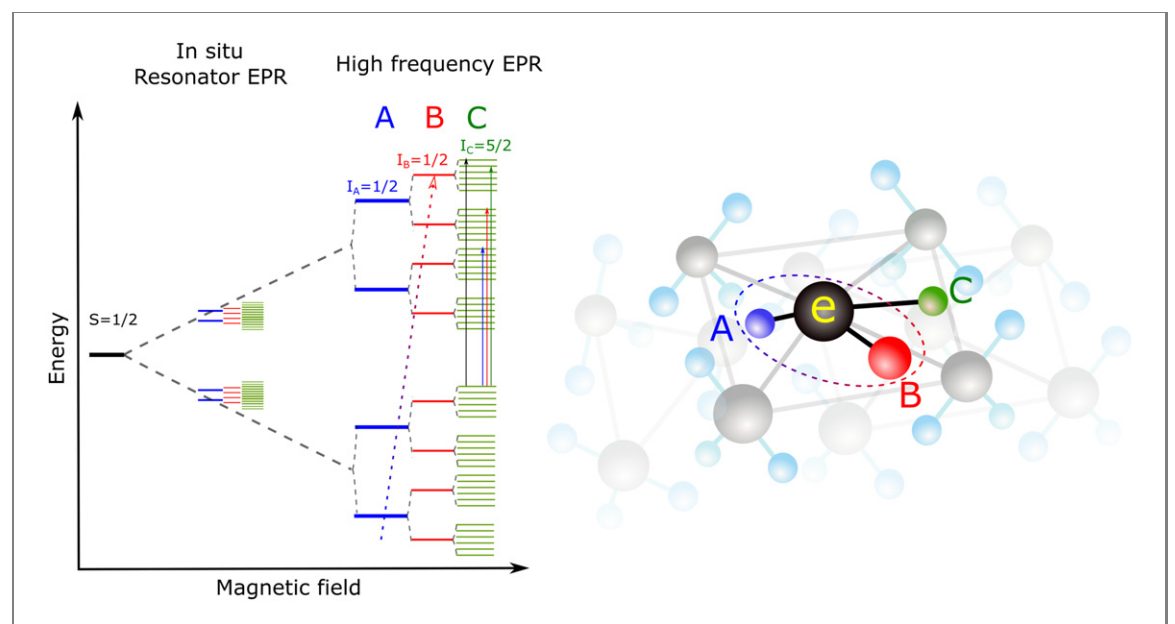


**Figure 3.** Chemical and structural identification through EPR. Large magnetic fields give increased level separation, and weakly coupled nuclear spins can be resolved and acquired spectra can be matched to density functional theory (DFT) calculations to precisely determine the structure of the electronic defect. Indicated is an electron spin transition (black arrow) of a fictitious defect sketched on the right, transitions involving an individual nuclear and an electron spin (colored arrows) and a multi-nuclear transition in ELDOR-NMR which can be used to associate multiple nuclei to the same electron spin (dashed arrow).

In general, detailed electronic structure of radicals can be obtained from pulsed EPR-based nuclear hyperfine spectroscopy [97]. Electron spin echo envelope modulation and electron-nuclear double resonance (ENDOR) are the two most commonly used techniques [98]. At high frequencies and magnetic-fields, electron-double resonance detected NMR (ELDOR-NMR) probing simultaneous nuclear and electron spin transitions (figure 3) is a particularly effective tool for studying hyperfine and nuclear quadrupolar interactions of nuclear spin with low gyromagnetic ratios and is sufficiently sensitive to detect nuclei with low natural abundance. ELDOR-NMR can also be used to correlate nuclei, that is identify nuclear spins belonging to a common paramagnetic center by simultaneously driving multiple nuclear transitions. The nuclear hyperfine and quadrupolar interactions measured by these techniques can be combined with values from DFT calculations. This approach has the benefit that computational modeling and interpretation of the measurements mutually constrain each other, leading to more reliable models of the electronic structure of the paramagnetic centers. For example, <sup>27</sup>Al and <sup>1</sup>H ENDOR and ELDOR-NMR combined with DFT modeling indicated that the unpaired electrons of  $\alpha$ -Al<sub>2</sub>O<sub>3</sub> surface radicals were largely localized to two aluminum atoms and the surface oxygens to which they were bound [96]. Two large proton hyperfine interactions arose from protons bonded to the surface oxygen. This extended knowledge about the radical and its environment from ex situ high-field EPR and DFT modeling could then be correlated with the earlier in situ EPR response obtained with superconducting resonators. In this way, quantum device performance can be associated with a chemical and structural identity of specific defects.

This type of high-field EPR approach provides a foundation for measurements on other materials and structures involving other nuclei, notably <sup>29</sup>Si and <sup>93</sup>Nb in oxides common to superconducting quantum devices. 240 GHz high-field EPR and <sup>93</sup>Nb ENDOR have already been demonstrated on Cr<sup>5+</sup>-doped K<sub>3</sub>NbO<sub>8</sub>, a candidate for an electron spin qubit [98]. Recently, 95 GHz <sup>29</sup>Si and <sup>13</sup>C ENDOR studies on spin-3/2 color centers in SiC were reported [99]. We anticipate that more sophisticated DFT approaches involving the crystalline nature of the materials will further enhance the use of high-field EPR for studying materials used in superconducting quantum circuits.

An interesting property of metal oxide surfaces is the presence of charge donor and acceptor sites. Characterisation of these sites using functionalisation and EPR detection on various polymorphs of  $Al_2O_3$  crystals consistently find a density of charge donor sites of  $10^{16}-10^{17}$  m<sup>-2</sup> [100–102], similar to the density of paramagnetic species thought to be responsible for flux noise [22]. Similar techniques might be of use for quantum circuits—where specific EPR active molecules can functionalzse the surface and be used as probes of the local environment of donor sites on  $Al_2O_3$  [103] and other metal oxides.

# 6. Characterising individual TLS

In what follows, we will now discuss various methods that are capable of interrogating individual TLSs one by one. This may provide an alternative approach to the aforementioned methods in order to connect the *in situ* detection of TLS with structural or chemical information obtained using 'classical' surface science.

#### 6.1. In situ device measurements

The extreme sensitivity of superconducting quantum circuits to the presence of even a small number of TLSs can be exploited in experiments designed to study the properties of individual TLSs. Here, we will only give a brief overview, and we refer to a recent review for a more detailed discussion [1].

In recent years, experiments with quantum circuits have introduced ways to directly tune the TLS energy to reveal more information about the TLSs that couple strongly to devices. The energy of an individual TLS can be written [9, 104] as,

$$E = \hbar \sqrt{\Delta^2 + \left(\epsilon + \frac{2pE}{\hbar} + \frac{2\gamma\xi}{\hbar}\right)^2},\tag{1}$$

where  $\epsilon$  is the intrinsic asymmetry energy, p the electric dipole moment,  $\gamma$  the elastic dipole moment and  $\xi$  the elastic field. Thus, by introducing an external electric or elastic field we can tune the energy of the TLS allowing us to directly obtain information about TLS energies and dipole moments [105] as well as TLS relaxation and dephasing times [11]. Experiments on macroscopic devices typically reveal a large number of hyperbolas described by equation (1) giving information about parameter distributions [104, 106], TLS relaxation times [11] and individual TLS–TLS couplings [107] can sometimes also be observed. This selectivity permits studying TLS dynamics; the parameters of TLS themselves constantly drift over time and the timescales involved can be very long. Changes that take place over days or even longer have been observed in experiments that probe the frequency  $\omega_{\text{TLS}} = E/\hbar$  of individual TLSs [2, 18, 19, 108, 109]. The detected TLSs can also be used as sensors to reveal information about the very low energy excitations (cf thermal fluctuators in figure 1) [108, 110] that govern the dynamics of coherent TLS and the low-frequency noise and dephasing in devices [84, 111].

Two important extensions to this method include time-varying tuning and the application of directional fields. A time-varying electrical field can be applied using external electrodes orspecially designed lumped superconducting resonators where the TLSs in a material under study are situated in a parallel-plate capacitor [105]. The latter method allows for a high-frequency field to be applied, which can give rise to interesting dynamics and allows one to determine average TLS parameters [112]. The use of directional fields has recently been demonstrated using (multiple) gating electrodes in the sample enclosure [108, 113] and in combination with strain tuning [23, 24, 114]. This is an effective way to map out the location of individual defects with respect to well-defined features of the device geometry.

These techniques are rapidly developing, and they provide access to TLS properties, such as dipole moment, energies, switching dynamics, spectral diffusion and device couplings. However, they are not capable of revealing direct structural or chemical information about the defects. This could potentially be overcome by utilising more localized fields, for example, using scanning probe microscopy (SPM).

## 6.2. Scanning probe microscopy techniques

SPM techniques, typically based on scanning tunneling microscopy (STM) or AFM, and both offering atomic resolution can offer a route towards individual TLS detection. Developing SPM techniques capable of interrogating quantum coherence is becoming an increasingly important challenge for materials science [115]. Here, we will give a brief overview of various SPM techniques that could potentially be developed to link individual TLSs to chemical or structural information.

STM is approaching energy resolution comparable to coherent TLS energies [116]. However, energy resolution is ultimately limited to the low  $\mu$ eV [117], although shot-noise spectroscopy with STM can potentially probe even lower energy processes [118]. STM was recently used to study granular Al and the presence of subgap Yu–Shiba–Rusinov (YSR) states might be related to unpaired electrons in the oxide [119]. YSR states are bound states within the superconducting gap that forms due to magnetic impurities, which in the limit of high but weakly coupled spin densities results in the formation of sub-gap impurity bands [120]. These could contribute to quasiparticle trapping, local gap fluctuations and increased surface impedance, and could potentially affect TLS dynamics [108]. Recent STM experiments on  $InO_x$  indicate that surface magnetic disorder arises from YSR states intrinsic to the superconductor surface, possibly from dangling bonds [121]. On the other hand, techniques that combine ESR with STM using a spin-polarized STM tip can access magnetic ground-state information and measurements of spin dynamics on the atomic scale [122–124]. However, the

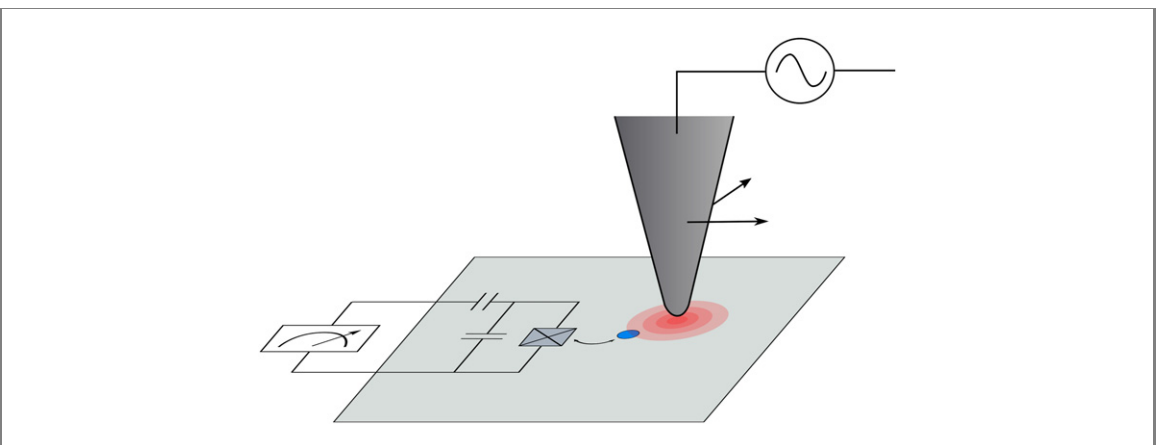


**Figure 4.** Quantum SPM to reveal TLS properties. Quantum circuit in operation couples to a TLS defect (blue dot) that is locally interacting with a nanoscale scanning probe.

drawback with all STM-based techniques is that they require conducting samples and cannot be used on metals with thick oxides or on dielectric substrates.

Alternatively, AFM, a standard tool to investigate surface roughness of thin films and substrates, can image any surface. State-of-the-art techniques can probe the connection between surface dissipation and static variations in the surface potential [125], which might link to surface TLS. An advantage of AFM is that it can be combined with a wide range of other techniques and readout schemes, where the AFM is mainly used to maintain a constant tip-sample separation.

#### 6.3. Scanning with quantum sensors

A range of these scanning probe techniques exist that exploit quantum phenomena or quantum devices as probes: scanning SQUIDs with single-spin sensitivity [126], scanning single-electron transistors [127] achieving sub-electron charge sensitivity, scanning Hall bars [128], cold-atom microscopes [129], Josephson junction microscopes [130], scanning quantum dot microscopy [131] and scanning nitrogen vacancy (NV) microscopy [132]. These techniques are mainly sensitive probes of local magnetic or electric fields, and not primary probes of the local coherence properties or TLS couplings. Only the latter exploits quantum two-level systems for both magnetic field [132] and electric field [133] sensing. Surface NMR with NV centers in diamond is also emerging as a powerful technique to reveal the chemical information and reaction chemistry of surfaces, and can for example be applied to study hydroxylation of Al<sub>2</sub>O<sub>3</sub> surfaces [134]. NV magnetometry can be performed either in a scanning probe configuration [132] or by addressing individual NV centers close to a coated diamond surface [135]. The drawback is the optically detected readout, which prevents ultralow temperature applications relevant for TLSs, and while sensitive to very small energy scales, on its own this technique could not directly identify TLS defects as they appear in quantum circuits.

Instead, drawing upon the strength of quantum circuits being very sensitive to TLS, the most natural way to locate individual TLS with nanoscale precision would be to use the same circuits as scanning probes. Furthermore, the non-uniform electric field distribution from a nanoscale probe would result in spatially non-uniform coupling to a TLS, revealing its orientation, which could be correlated with material structural information obtained through e.g. AFM or other surface analysis techniques.

There have been a few theoretical proposals that discuss the possibility of using quantum circuits in an SPM configuration to interrogate nanoscale material properties. This includes charge qubit on a tip [136, 137] and quantum harmonic oscillators [138]. Experimental implementations are scarce at present. A notable example is the scanning transmon [139] that could be used as a probe of local coherence and potentially TLS detection. In the same way, one can imagine scanning with a well-placed TLS defect on a tip (given an appropriate readout circuit), which would be an atomic scale equivalent of a scanning qubit. This TLS would be able to interact with other TLSs in the sample, revealing information about them.

The simplest quantum circuit possible for TLS detection would be an harmonic oscillator in the quantum regime, such as a superconducting resonator operating at microwave frequencies [140], essentially extending the common technique of near-field microwave microscopy to the quantum regime [141]. It is shown that a nanometer-sized metallic tip in this case can reach the strong coupling regime with a TLS on the surface [138].

Another interesting experiment was recently demonstrated on a semiconductor spin qubit [142]. Here, scanning gate microscopy was used to map the electric field profile of the device, where the device charge state is monitored *in situ* as a function of tip location and bias. This local electric field spectroscopy is able

to map imperfections in the local electric field distributions of the device, arising from, e.g. fabrication imperfections or charge defects. Similar local perturbation was demonstrated on a lattice of superconducting resonators [143].

In order to unlock the potential of 'quantum' SPM techniques advances still have to be made in cryogenic SPM engineering, as to date no SPM platform has demonstrated high-coherence operation of a quantum circuit (e.g. on the sample stage) at mK temperatures ([139, 141] are to our knowledge the most 'coherent' SPM platforms for superconducting circuits described to date). Another complication is achieving a stable (vibration-free) environment, as any mechanical noise will directly translate into fluctuations of the coupling strength between the probe and TLS. Despite these significant experimental challenges, a 'quantum' SPM either imaging with a quantum circuit or hosting one on the sample stage for *in situ* TLS detection, as sketched in figure 4, would provide the missing link that allows one to directly correlate individually observed and localiszd TLS defects with other surface science techniques.

#### 7. Conclusion

The physics of TLSs and their effects on quantum circuits have turned out to be far richer and more complicated than anyone expected. It is now clear that solving this problem, thereby enabling a range of important applications, will require the combined efforts of the materials science and quantum circuit communities.

To unlock the full potential of surface analysis techniques for superconducting quantum circuits we will need new techniques that (i) can detect individual TLS defects as and where they appear in circuits and (ii) are able to correlate or directly link these with structural or chemical information that is also accessible to well-established surface analysis techniques. Bridging this gap will require one to explore a wide range of correlative surface science, treatments and materials as well as to develop new techniques capable of *in situ* device measurements that can reveal the exact locations, chemistry and structure of defects. We envisage that this will be possible, for example, by the development of new versatile quantum scanning probe techniques that can identify the same defect using several scanning modes, and with further developments in *in situ* EPR techniques and device treatments.

We also know that surfaces and interfaces are highly complex and trying to explain TLS by a single type of chemical or structural entity is likely to fail. Instead, it is more probable that the decoherence arises from a complex cocktail of surface defects with many different origins, and they need to be eliminated one by one. However, revealing and subsequently mitigating the most prominent ones will hopefully lead to significant device improvements over time.

The need for better materials for quantum technologies is now driven by the rapidly growing quantum computing industry and this will undoubtedly drive the development of new characterisation tools in the coming years, specifically tailored towards addressing the materials challenge for quantum circuits.

# Acknowledgments

This work was supported by the UK government Department for Business, Energy and Industrial Strategy through the UK national quantum technologies program. SdG acknowledges support by the Engineering and Physical Sciences Research Council (EPSRC) (Grant Number EP/W027526/1). SU is grateful for support from the DRF-Impulsion Program of the CEA and the DIM-ELICIT and SESAME programs of the Région Ile-de-France.

### Data availability statement

No new data were created or analyzed in this study.

#### **ORCID** iDs

S E de Graaf https://orcid.org/0000-0001-9815-8030
S Un https://orcid.org/0000-0001-7032-2433
A G Shard https://orcid.org/0000-0002-8931-5740
T Lindstróm https://orcid.org/0000-0003-1861-6551

#### References

[1] Müller C, Cole J H and Lisenfeld J 2019 Towards understanding two-level-systems in amorphous solids: insights from quantum circuits Rep. Prog. Phys. 82 124501

- [2] Klimov P V et al 2018 Fluctuations of energy-relaxation times in superconducting qubits Phys. Rev. Lett. 121 090502
- [3] de Leon N P et al 2021 Materials challenges and opportunities for quantum computing hardware Science 372 abb2823
- [4] Dutta P and Horn P M 1981 Low-frequency fluctuations in solids: 1/f noise Rev. Mod. Phys. 53 497
- [5] Martinis J M et al 2005 Decoherence in Josephson qubits from dielectric loss Phys. Rev. Lett. 95 210503
- [6] Astafiev O, Pashkin Y, Nakamura Y, Yamamoto T and Tsai J 2004 Quantum noise in the Josephson charge qubit Phys. Rev. Lett. 93 267007
- [7] Yoshihara F, Harrabi K, Niskanen A O, Nakamura Y and Tsai J S 2006 Decoherence of flux qubits due to 1/f flux noise Phys. Rev. Lett. 97 167001
- 8] Neeley M et al 2008 Process tomography of quantum memory in a Josephson-phase qubit coupled to a two-level state Nat. Phys. 4 523–6
- [9] Phillips W A 1987 Two-level states in glasses Rep. Prog. Phys. 50 1657
- [10] Grabovskij G J, Peichl T, Lisenfeld J, Weiss G and Ustinov A V 2012 Strain tuning of individual atomic tunneling systems detected by a superconducting qubit Science 338 232-4
- [11] Lisenfeld J et al 2016 Decoherence spectroscopy with individual two-level tunneling defects Sci. Rep. 6 23786
- [12] Weides M P, Kline J S, Vissers M R, Sandberg M O, Wisbey D S, Johnson B R, Ohki T A and Pappas D P 2011 Coherence in a transmon qubit with epitaxial tunnel junctions *Appl. Phys. Lett.* 99 262502
- [13] Bruno A, de Lange G, Asaad S, van der Enden K L, Langford N K and DiCarlo L 2015 Reducing intrinsic loss in superconducting resonators by surface treatment and deep etching of silicon substrates Appl. Phys. Lett. 106 182601
- [14] Calusine G et al 2018 Analysis and mitigation of interface losses in trenched superconducting coplanar waveguide resonators Appl. Phys. Lett. 112 062601
- [15] Woods W, Calusine G, Melville A, Sevi A, Golden E, Kim D K, Rosenberg D, Yoder J L and Oliver W D 2019 Determining interface dielectric losses in superconducting coplanar-waveguide resonators *Phys. Rev. Appl.* 12 014012
- [16] Richardson C J K, Lordi V, Misra S and Shabani J 2020 Materials science for quantum information science and technology MRS Bull. 45 485–97
- [17] Siddiqi I 2021 Engineering high-coherence superconducting qubits Nat. Rev. Mater. 6 875
- [18] Béjanin J H, Earnest C T, Sharafeldin A S and Mariantoni M 2021 Interacting defects generate stochastic fluctuations in superconducting qubits *Phys. Rev.* B 104 094106
- [19] Burnett J J, Bengtsson A, Scigliuzzo M, Niepce D, Kudra M, Delsing P and Bylander J 2019 Decoherence benchmarking of superconducting qubits npj Quantum Inf. 5 54
- [20] Carroll M, Rosenblatt S, Jurcevic P, Lauer I and Kandala A 2021 Dynamics of superconducting qubit relaxation times (arXiv:2105.15201)
- [21] Kumar P et al 2016 Origin and suppression of 1/f magnetic flux noise Phys. Rev. Appl. 6 041001
- [22] Sendelbach S, Hover D, Kittel A, Mück M, Martinis J M and McDermott R 2008 Magnetism in squids at millikelvin temperatures Phys. Rev. Lett. 100 227006
- [23] Lisenfeld J, Bilmes A, Megrant A, Barends R, Kelly J, Klimov P, Weiss G, Martinis J M and Ustinov A V 2019 Electric field spectroscopy of material defects in transmon qubits npj Quantum Inf. 5 105
- [24] Bilmes A, Volosheniuk S, Ustinov A V and Lisenfeld J 2022 Probing defect densities at the edges and inside Josephson junctions of superconducting qubits npj Quantum Inf. 8 24
- [25] de Graaf S E, Adamyan A A, Lindstróm T, Erts D, Kubatkin S E, Tzalenchuk A Y and Danilov A V 2017 Direct identification of dilute surface spins on Al<sub>2</sub>O<sub>3</sub>: origin of flux noise in quantum circuits Phys. Rev. Lett. 118 057703
- [26] Holder A M, Osborn K D, Lobb C J and Musgrave C B 2013 Bulk and surface tunneling hydrogen defects in alumina Phys. Rev. Lett. 111 065901
- [27] Wang Z, Wang H, Yu C C and Wu R Q 2018 Hydrogen as a source of flux noise in squids Phys. Rev. B 98 020403
- [28] Lee D, DuBois J L and Lordi V 2014 Identification of the local sources of paramagnetic noise in superconducting qubit devices fabricated on  $\alpha$ -Al<sub>2</sub>O<sub>3</sub> substrates using density-functional calculations *Phys. Rev. Lett.* 112 017001
- [29] Wang C, Axline C, Gao Y Y, Brecht T, Chu Y, Frunzio L, Devoret M H and Schoelkopf R J 2015 Surface participation and dielectric loss in superconducting qubits Appl. Phys. Lett. 107 162601
- [30] Kim S, Terai H, Yamashita T, Qiu W, Fuse T, Yoshihara F, Ashhab S, Inomata K and Semba K 2021 Enhanced coherence of all-nitride superconducting qubits epitaxially grown on silicon substrate *Commun. Mater.* 2 98
- [31] Chang J B, Gibson G W and Ketchen M B 2015 Trilayer Josephson junction structure with small air bridge and no interlevel dielectric for superconducting qubits U.S. Patent US9564573B1 https://patents.google.com/patent/US9564573B1/en
- [32] Zhao R, Park S, Zhao T, Bal M, McRae C R H, Long J and Pappas D P 2020 Merged-element transmon Phys. Rev. Appl. 14 064006
- [33] Wang J I-J et al 2019 Coherent control of a hybrid superconducting circuit made with graphene-based van der Waals heterostructures Nat. Nanotechnol. 14 120–5
- [34] Antony A, Gustafsson M V, Rajendran A, Benyamini A, Ribeill G, Ohki T A, Hone J and Fong K C 2022 Making high-quality quantum microwave devices with van der Waals superconductors J. Phys.: Condens. Matter 34 103001
- [35] Place A P M et al 2021 New material platform for superconducting transmon qubits with coherence times exceeding 0.3 milliseconds Nat. Commun. 12 1779
- [36] Wang C et al 2022 Towards practical quantum computers: transmon qubit with a lifetime approaching 0.5 milliseconds npj Quantum Inf. 8 3
- [37] Deng H et al 2022 Titanium nitride film on sapphire substrate with low dielectric loss for superconducting qubits (arXiv:2205.03528)
- [38] Fu Q, Wagner T and Rühle M 2006 Hydroxylated α-Al<sub>2</sub>O<sub>3</sub> (0001) surfaces and metal/α-Al<sub>2</sub>O<sub>3</sub> (0001) interfaces Surf. Sci. 600 4870-7
- [39] Mergenthaler M et al 2021 Effects of surface treatments on flux tunable transmon qubits npj Quantum Inf. 7 157
- [40] Mergenthaler M et al 2021 Ultrahigh vacuum packaging and surface cleaning for quantum devices Rev. Sci. Instrum. 92 025121
- [41] Earnest C T, Béjanin J H, McConkey T G, Peters E A, Korinek A, Yuan H and Mariantoni M 2018 Substrate surface engineering for high-quality silicon/aluminum superconducting resonators *Supercond. Sci. Technol.* 31 125013
- [42] Shard A G 2014 Detection limits in XPS for more than 6000 binary systems using Al and Mg K $\alpha$  x-rays Surf. Interface Anal. 46
- [43] Odobesko A B et al 2019 Preparation and electronic properties of clean superconducting Nb(110) surfaces Phys. Rev. B 99 115437

- [44] Uhart A, Ledeuil J B, Pecquenard B, Le Cras F, Proust M and Martinez H 2017 Nanoscale chemical characterization of solid-state microbattery stacks by means of auger spectroscopy and ion-milling cross section preparation ACS Appl. Mater. Interfaces 9 33238–49
- [45] King P D C, Picozzi S, Egdell R G and Panaccione G 2021 Angle, spin, and depth resolved photoelectron spectroscopy on quantum materials Chem. Rev. 121 2816–56
- [46] Afanas'ev V P, Gryazev A S, Efremenko D S, Kaplya P S and Ridzel O Y 2016 Determination of atomic hydrogen in hydrocarbons by means of the reflected electron energy loss spectroscopy and the x-ray photoelectron spectroscopy J. Phys.: Conf. Ser. 748 012005
- [47] Vos M, Liu X, Grande P L, Nandi S K, Venkatachalam D K and Elliman R G 2014 The use of electron Rutherford backscattering to characterize novel electronic materials as illustrated by a case study of sputter-deposited NbO<sub>x</sub> films *Nucl. Instrum. Methods Phys. Res.* B 340 58–62
- [48] Kowsari D, Zheng K, Monroe J T, Thobaben N J, Du X, Harrington P M, Henriksen E A, Wisbey D S and Murch K W 2021 Fabrication and surface treatment of electron-beam evaporated niobium for low-loss coplanar waveguide resonators Appl. Phys. Lett. 119 132601
- [49] Altoé M V P et al 2022 Localization and mitigation of loss in niobium superconducting circuits PRX Quantum 3 020312
- [50] Verjauw J et al 2020 Investigation of microwave loss induced by oxide regrowth in high-q Nb resonators Phys. Rev. Appl. 16 014018
- [51] Davies T, Grovenor C R M and Speller S C 2020 Atmospheric oxidation of NbTi superconductor J. Alloys Compd. 848 156345
- [52] Melville A et al 2020 Comparison of dielectric loss in titanium nitride and aluminum superconducting resonators Appl. Phys. Lett. 117 124004
- [53] Zheng K, Kowsari D, Thobaben N J, Du X, Song X, Ran S, Henriksen E A, Wisbey D S and Murch K W 2022 Nitrogen plasma passivated niobium resonators for superconducting quantum circuits Appl. Phys. Lett. 120 102601
- [54] Mosenfelder J L, Le Voyer M, Rossman G R, Guan Y, Bell D R, Asimow P D and Eiler J M 2011 Analysis of hydrogen in olivine by SIMS: evaluation of standards and protocol Am. Mineral. 96 1725–41
- [55] Sandberg M, Adiga V P, Brink M, Kurter C, Murray C, Hopstaken M, Bruley J, Orcutt J S and Paik H 2021 Investigating microwave loss of SiGe using superconducting transmon qubits Appl. Phys. Lett. 118 124001
- [56] Richardson C J K, Alexander A, Weddle C G, Arey B and Olszta M 2020 Low-loss superconducting titanium nitride grown using plasma-assisted molecular beam epitaxy *J. Appl. Phys.* 127 235302
- [57] Romanenko A, Pilipenko R, Zorzetti S, Frolov D, Awida M, Belomestnykh S, Posen S and Grassellino A 2020 Three-dimensional superconducting resonators at t < 20 mK with photon lifetimes up to  $\tau = 2$  s *Phys. Rev. Appl.* 13 034032
- [58] McRae C R H, Béjanin J H, Earnest C T, McConkey T G, Rinehart J R, Deimert C, Thomas J P, Wasilewski Z R and Mariantoni M 2018 Thin film metrology and microwave loss characterization of indium and aluminum/indium superconducting planar resonators J. Appl. Phys. 123 205304
- [59] Murthy A A, Lee J, Kopas C, Reagor M J, McFadden A P, Pappas D P, Checchin M, Grassellino A and Romanenko A 2022 TOF-SIMS analysis of decoherence sources in superconducting qubits Appl. Phys. Lett. 120 044002
- [60] Lee J, Sung Z, Murthy A A, Reagor M J, Grassellino A and Romanenko A 2021 Discovery of Nb hydride precipitates in superconducting qubits (arXiv:2108.10385)
- [61] Jasim A M, He X, Xing Y, White T A and Young M J 2021 Cryo-ePDF: overcoming electron beam damage to study the local atomic structure of amorphous ALD aluminum oxide thin films within a TEM ACS Omega 6 8986–9000
- [62] Zeng L J, Nik S, Greibe T, Krantz P, Wilson C M, Delsing P and Olsson E 2015 Direct observation of the thickness distribution of ultra thin AlO<sub>x</sub> barriers in Al/AlO<sub>x</sub>/Al Josephson junctions *J. Phys. D: Appl. Phys.* 48 395308
- [63] Zeng L J, Krantz P, Nik S, Delsing P and Olsson E 2015 The atomic details of the interfacial interaction between the bottom electrode of Al/AlO<sub>x</sub>/Al Josephson junctions and HF-treated Si substrates *J. Appl. Phys.* 117 163915
- [64] Fritz S, Seiler A, Radtke L, Schneider R, Weides M, Weiß G and Gerthsen D 2018 Correlating the nanostructure of Al-oxide with deposition conditions and dielectric contributions of two-level systems in perspective of superconducting quantum circuits Sci. Rep. 8 7956
- [65] Fritz S, Radtke L, Schneider R, Weides M and Gerthsen D 2019 Optimization of Al/AlO<sub>x</sub>/Al-layer systems for Josephson junctions from a microstructure point of view J. Appl. Phys. 125 165301
- [66] Verjauw J et al 2022 Path toward manufacturable superconducting qubits with relaxation times exceeding 0.1 ms (arXiv:2022.10303)
- [67] Quintana C M et al 2014 Characterization and reduction of microfabrication-induced decoherence in superconducting quantum circuits Appl. Phys. Lett. 105 062601
- [68] Richardson C J K, Siwak N P, Hackley J, Keane Z K, Robinson J E, Arey B, Arslan I and Palmer B S 2016 Fabrication artifacts and parallel loss channels in metamorphic epitaxial aluminum superconducting resonators *Supercond. Sci. Technol.* 29 064003
- [69] Murthy A A et al 2022 Potential nanoscale sources of decoherence in niobium based transmon qubit architectures (arXiv:2203.08710)
- [70] Barkov F, Romanenko A and Grassellino A 2012 Direct observation of hydrides formation in cavity-grade niobium Phys. Rev. ST Accel. Beams 15 122001
- [71] Romanenko A, Barkov F, Cooley L D and Grassellino A 2013 Proximity breakdown of hydrides in superconducting niobium cavities Supercond. Sci. Technol. 26 035003
- [72] Sheridan E, Harrelson T F, Sivonxay E, Persson K A, Altoé M V P, Siddiqi I, Ogletree D F, Santiago D I and Griffin S M 2021 Microscopic theory of magnetic disorder-induced decoherence in superconducting Nb films (arXiv:2111.11684)
- [73] Harrelson T F et al 2021 Elucidating the local atomic and electronic structure of amorphous oxidized superconducting niobium films Appl. Phys. Lett. 119 244004
- [74] Premkumar A et al 2021 Microscopic relaxation channels in materials for superconducting qubits Commun. Mater. 2 72
- [75] Foxen B et al 2017 Qubit compatible superconducting interconnects Quantum Sci. Technol. 3 014005
- [76] Hass K C, Schneider W F, Curioni A and Andreoni W 1998 The chemistry of water on alumina surfaces: reaction dynamics from first principles *Science* 282 265–8
- [77] Sung J, Zhang L, Tian C, Waychunas G A and Shen Y R 2011 Surface structure of protonated R-sapphire (1102) studied by sum-frequency vibrational spectroscopy *J. Am. Chem. Soc.* 133 3846–53
- [78] Nguyen L, Hashimoto T, Zakharov D N, Stach E A, Rooney A P, Berkels B, Thompson G E, Haigh S J and Burnett T L 2018 Atomic-scale insights into the oxidation of aluminum ACS Appl. Mater. Interfaces 10 2230–5

- [79] Lu Y-H and Chen H-T 2015 Hydrogen generation by the reaction of H<sub>2</sub>O with Al<sub>2</sub>O<sub>3</sub>-based materials: a computational analysis Phys. Chem. Chem. Phys. 17 6834
- [80] Jenness G R, Christiansen M A, Caratzoulas S, Vlachos D G and Gorte R J 2014 Site-dependent Lewis acidity of  $\gamma$ -Al<sub>2</sub>O<sub>3</sub> and its impact on ethanol dehydration and etherification *J. Phys. Chem.* C **118** 12899–907
- 81] Micke P et al 2019 Closed-cycle, low-vibration 4 K cryostat for ion traps and other applications Rev. Sci. Instrum. 90 065104
- [82] de Graaf S E, Faoro L, Burnett J, Adamyan A A, Tzalenchuk A Y, Kubatkin S E, Lindstróm T and Danilov A V 2018 Suppression of low-frequency charge noise in superconducting resonators by surface spin desorption Nat. Commun. 9 1143
- [83] Burnett J, Faoro L and Lindstróm T 2016 Analysis of high quality superconducting resonators: consequences for TLS properties in amorphous oxides Supercond. Sci. Technol. 29 044008
- [84] Faoro L and Ioffe L B 2015 Interacting tunneling model for two level systems in amorphous materials and its predictions for their dephasing and noise in superconducting microresonators Phys. Rev. B 91 014201
- [85] Stutzmann M and Biegelsen D K 1983 Electron-spin-lattice relaxation in amorphous silicon and germanium Phys. Rev. B 28 6256
- [86] Askew T R, Stapleton H J and Brower K L 1986 Anomalous electron-spin relaxation in amorphous silicon Phys. Rev. B 33 4455
- 87] Belli M, Fanciulli M and de Sousa R 2020 Probing two-level systems with electron spin inversion recovery of defects at the Si/SiO<sub>2</sub> interface Phys. Rev. Res. 2 033507
- 88] Morton JJL and Bertet P 2018 Storing quantum information in spins and high-sensitivity ESR J. Magn. Reson. 287 128-39
- [89] Kubo Y et al 2011 Hybrid quantum circuit with a superconducting qubit coupled to a spin ensemble Phys. Rev. Lett. 107 220501
- [90] Ranjan V, Probst S, Albanese B, Schenkel T, Vion D, Esteve D, Morton J J L and Bertet P 2020 Electron spin resonance spectroscopy with femtoliter detection volume Appl. Phys. Lett. 116 184002
- [91] Samkharadze N, Bruno A, Scarlino P, Zheng G, DiVincenzo D P, DiCarlo L and Vandersypen L M K 2016 High kinetic inductance superconducting nanowire resonators for circuit OED in a magnetic field *Phys. Rev. Appl.* 5 044004
- [92] Borisov K et al 2020 Superconducting granular aluminum resonators resilient to magnetic fields up to 1 tesla Appl. Phys. Lett. 117 120502
- [93] Lenahan P M and Conley J F Jr 1998 What can electron paramagnetic resonance tell us about the Si/SiO<sub>2</sub> system? J. Vac. Sci. Technol. B 16 2134
- [94] Pierreux D and Stesmans A 2002 Frequency-dependent electron spin resonance study of P<sub>b</sub>-type interface defects in thermal Si/SiO<sub>2</sub> Phys. Rev. B 66 165320
- [95] Jones B J and Barklie R C 2005 Electron paramagnetic resonance evaluation of defects at the (100)Si/Al<sub>2</sub>O<sub>3</sub> interface J. Phys. D: Appl. Phys. 38 1178–81
- [96] Un S, de Graaf S E, Bertet P, Kubatkin S E and Danilov A V 2022 On the nature of decoherence in quantum circuits: revealing the structural motif of the surface radicals in α-Al<sub>2</sub>O<sub>3</sub> Sci. Adv. 8 eabm6169
- [97] Chiesa M, Giamello E and Che M 2009 EPR characterization and reactivity of surface-localized inorganic radicals and radical ions Chem. Rev. 110 1320–47
- [98] Nellutla S, Morley G W, van Tol J, Pati M and Dalal N S 2008 Electron spin relaxation and <sup>39</sup>K pulsed ENDOR studies on Cr<sup>5+</sup>-doped K<sub>3</sub>NbO<sub>8</sub> at 9.7 and 240 GHz *Phys. Rev.* B **78** 054426
- [99] Soltamov V A, Yavkin B V, Mamin G V, Orlinskii S B, Breev I D, Bundakova A P, Babunts R A, Anisimov A N and Baranov P G 2021 Electron nuclear interactions in spin-3/2 color centers in silicon carbide: a high-field pulse EPR and ENDOR study *Phys. Rev.* B 104 125205
- [100] Gafurov M R, Mukhambetov I N, Yavkin B V, Mamin G V, Lamberov A A and Orlinskii S B 2015 Quantitative analysis of Lewis acid centers of γ-alumina by using EPR of the adsorbed anthraquinone as a probe molecule: comparison with the pyridine, carbon monoxide IR, and TPD of ammonia J. Phys. Chem. C 119 27410-5
- [101] Medvedev D A, Rybinskaya A A, Kenzhin R M, Volodin A M and Bedilo A F 2012 Characterization of electron donor sites on Al<sub>2</sub>O<sub>3</sub> surface Phys. Chem. Chem. Phys. 14 2587–98
- [102] Bedilo A F, Shuvarakova E I, Rybinskaya A A and Medvedev D A 2014 Characterization of electron-donor and electron-acceptor sites on the surface of sulfated alumina using spin probes J. Phys. Chem. C 118 15779–94
- [103] Mukhambetov I N, Lamberov A A, Yavkin B V, Gafurov M R, Mamin G V and Orlinskii S B 2014 Electron paramagnetic resonance and electron nuclear double resonance study of the paramagnetic complexes of anthraquinone on the surface of  $\gamma$ -Al<sub>2</sub>O<sub>3</sub> *J. Phys. Chem.* C 118 14998–5003
- [104] Carruzzo H M, Bilmes A, Lisenfeld J, Yu Z, Wang B, Wan Z, Schmidt J R and Yu C C 2021 Distribution of two-level system couplings to strain and electric fields in glasses at low temperatures *Phys. Rev.* B 104 134203
- [105] Sarabi B, Ramanayaka A N, Burin A L, Wellstood F C and Osborn K D 2016 Projected dipole moments of individual two-level defects extracted using circuit quantum electrodynamics Phys. Rev. Lett. 116 167002
- [106] Hung C-C, Yu L, Foroozani N, Fritz S, Gerthsen D and Osborn K D 2022 Probing hundreds of individual quantum defects in polycrystalline and amorphous alumina Phys. Rev. Appl. 17 034025
- [107] Lisenfeld J, Grabovskij G J, Müller C, Cole J H, Weiss G and Ustinov A V 2015 Observation of directly interacting coherent two-level systems in an amorphous material Nat. Commun. 6 6182
- [108] de Graaf S E, Mahashabde S, Kubatkin S E, Tzalenchuk A Y and Danilov A V 2021 Quantifying dynamics and interactions of individual spurious low-energy fluctuators in superconducting circuits *Phys. Rev.* B 103 174103
- [109] Schlór S, Lisenfeld J, Müller C, Bilmes A, Schneider A, Pappas D P, Ustinov A V and Weides M 2019 Correlating decoherence in transmon qubits: low frequency noise by single fluctuators *Phys. Rev. Lett.* **123** 190502
- [110] Meißner S M, Seiler A, Lisenfeld J, Ustinov A V and Weiss G 2018 Probing individual tunneling fluctuators with coherently controlled tunneling systems *Phys. Rev.* B 97 180505
- [111] Burin A L, Matityahu S and Schechter M 2015 Low-temperature 1/f noise in microwave dielectric constant of amorphous dielectrics in Josephson qubits Phys. Rev. B 92 174201
- [112] Yu L, Matityahu S, Rosen Y J, Hung C-C, Maksymov A, Burin A L, Schechter M and Osborn K D 2021 Evidence for weakly and strongly interacting two-level systems in amorphous silicon (arXiv:2110.10747)
- [113] Bilmes A, Megrant A, Klimov P, Weiss G, Martinis J M, Ustinov A V and Lisenfeld J 2020 Resolving the positions of defects in superconducting quantum bits Sci. Rep. 10 3090
- [114] Bilmes A, Volosheniuk S, Brehm J D, Ustinov A V and Lisenfeld J 2021 Quantum sensors for microscopic tunneling systems *npj* Quantum Inf. 7 1–6
- [115] Bian K, Gerber C, Heinrich A J, Müller D J, Scheuring S and Jiang Y 2021 Scanning probe microscopy *Nat. Rev. Methods Primers* 1 36

- [116] Fernández-Lomana M *et al* 2021 Millikelvin scanning tunneling microscope at 20/22 T with a graphite enabled stick-slip approach and an energy resolution below 8 µeV: application to conductance quantization at 20 T in single atom point contacts of Al and Au and to the charge density wave of 2H-NbSe<sub>2</sub> *Rev. Sci. Instrum.* 92 093701
- [117] Ast C R, Jäck B, Senkpiel J, Eltschka M, Etzkorn M, Ankerhold J and Kern K 2016 Sensing the quantum limit in scanning tunnelling spectroscopy *Nat. Commun.* 7 13009
- [118] Thupakula U U, Perrin V, Palacio-Morales A, Cario L, Aprili M, Simon P and Massee F 2022 Coherent and incoherent tunneling into Yu-Shiba-Rusinov states revealed by atomic scale shot-noise spectroscopy *Phys. Rev. Lett.* 128 247001
- [119] Yang F, Gozlinski T, Storbeck T, Grünhaupt L, Pop I M and Wulfhekel W 2020 Microscopic charging and in-gap states in superconducting granular aluminum Phys. Rev. B 102 104502
- [120] Fominov Y V, Houzet M and Glazman L I 2011 Surface impedance of superconductors with weak magnetic impurities Phys. Rev. B 84 224517
- [121] Tamir I, Trahms M, Gorniaczyk F, von Oppen F, Shahar D and Franke K J 2022 Direct observation of intrinsic surface magnetic disorder in amorphous superconducting films Phys. Rev. B 105 L140505
- [122] Loth S, Etzkorn M, Lutz C P, Eigler D M and Heinrich A J 2010 Measurement of fast electron spin relaxation times with atomic resolution *Science* 329 1628–30
- [123] van Weerdenburg W M J, Steinbrecher M, van Mullekom N P E, Gerritsen J W, von Allwórden H, Natterer F D and Khajetoorians A A 2021 A scanning tunneling microscope capable of electron spin resonance and pump-probe spectroscopy at mK temperature and in vector magnetic field Rev. Sci. Instrum. 92 033906
- [124] Seifert T S, Kovarik S, Gambardella P and Stepanow S 2021 Accurate measurement of atomic magnetic moments by minimizing the tip magnetic field in STM-based electron paramagnetic resonance (arXiv:2111.05043)
- [125] Héritier M, Pachlatko R, Tao Y, Abendroth J M, Degen C L and Eichler A 2021 Spatial correlation between fluctuating and static fields over metal and dielectric substrates Phys. Rev. Lett. 127 216101
- [126] Vasyukov D et al 2013 A scanning superconducting quantum interference device with single electron spin sensitivity Nat. Nanotechnol. 8 639–44
- [127] Yoo M J, Fulton T A, Hess H F, Willett R L, Dunkleberger L N, Chichester R J, Pfeiffer L N and West K W 1997 Scanning single-electron transistor microscopy: imaging individual charges Science 276 579–82
- [128] Chang A M et al 1992 Scanning Hall probe microscopy Appl. Phys. Lett. 61 1974
- [129] Gierling M, Schneeweiss P, Visanescu G, Federsel P, Häffner M, Kern D P, Judd T E, Günther A and Fortágh J 2011 Cold-atom scanning probe microscopy Nat. Nanotechnol. 6 446–51
- [130] Plourde B L T and van Harlingen D J 1999 Design of a scanning Josephson junction microscope for submicron-resolution magnetic imaging Rev. Sci. Instrum. 70 4344
- [131] Wagner C, Green M F B, Leinen P, Deilmann T, Krüger P, Rohlfing M, Temirov R and Tautz F S 2015 Scanning quantum dot microscopy Phys. Rev. Lett. 115 026101
- [132] Balasubramanian G et al 2008 Nanoscale imaging magnetometry with diamond spins under ambient conditions Nature 455
- [133] Bian K, Zheng W, Zeng X, Chen X, Stóhr R, Denisenko A, Yang S, Wrachtrup J and Jiang Y 2021 Nanoscale electric-field imaging based on a quantum sensor and its charge-state control under ambient condition *Nat. Commun.* 12 2457
- [134] Liu K S, Henning A, Heindl M W, Allert R D, Bartl J D, Sharp I D, Rizzato R and Bucher D B 2022 Surface NMR using quantum sensors in diamond *Proc. Natl Acad. Sci. USA* 119 2111607119
- [135] Staudacher T, Shi F, Pezzagna S, Meijer J, Du J, Meriles C A, Reinhard F and Wrachtrup J 2013 Nuclear magnetic resonance spectroscopy on a (5-nanometer) 3 sample volume *Science* 339 561–3
- [136] Jäck B 2020 Visualizing dissipative charge-carrier dynamics at the nanoscale with superconducting-charge-qubit microscopy Phys. Rev. Res. 2 043031
- [137] Khivrich I and Ilani S 2020 Atomic-like charge qubit in a carbon nanotube enabling electric and magnetic field nano-sensing Nat. Commun. 11 2299
- [138] de Graaf S E, Danilov A V and Kubatkin S E 2015 Coherent interaction with two-level fluctuators using near field scanning microwave microscopy Sci. Rep. 5 17176
- [139] Shanks W E, Underwood D L and Houck A A 2013 A scanning transmon qubit for strong coupling circuit quantum electrodynamics *Nat. Commun.* 4 1991
- [140] de Graaf S E, Danilov A V, Adamyan A and Kubatkin S E 2013 A near-field scanning microwave microscope based on a superconducting resonator for low power measurements Rev. Sci. Instrum. 84 023706
- [141] Geaney S, Cox D, Hónigl-Decrinis T, Shaikhaidarov R, Kubatkin S E, Lindstróm T, Danilov A V and de Graaf S E 2019 Near-field scanning microwave microscopy in the single photon regime *Sci. Rep.* **9** 12539
- [142] Oh S W, Denisov A O, Chen P and Petta J R 2021 Cryogen-free scanning gate microscope for the characterization of Si/Si<sub>0.7</sub>Ge<sub>0.3</sub> quantum devices at milli-kelvin temperatures AIP Adv. 11 125122
- [143] Underwood D L, Shanks W E, Li A C Y, Ateshian L, Koch J and Houck A A 2016 Imaging photon lattice states by scanning defect microscopy Phys. Rev. X 6 021044